$$\sum_{p=1}^{m} \beta_{pk}\langle E_r E_p^* \rangle = \delta_{rk}. \qquad (A4)$$

Multiplying both members of (A4) by β_{ks}^{-1} and summing over the index k, we obtain

$$\sum_{p=1}^{m}\left(\sum_{k=1}^{m} \beta_{pk}\beta_{ks}^{-1}\right)\langle E_r E_p^* \rangle = \langle E_r E_s^* \rangle = U_{rs} = \beta_{rs}^{-1}, \qquad (A5)$$

where the Sayre–Hughes equation (2.5) has been used. Therefore

$$\boldsymbol{\beta} = \mathbf{U}^{-1}, \qquad (A6)$$

which is (2.9) for the $P1$ case. The proof of the relation $\boldsymbol{\beta} = \frac{1}{2}\mathbf{U}^{-1}$ that holds in the $P\bar{1}$ case closely follows the same steps as in the $P1$ case.

References

BRILLOUIN, L. (1962). *Science and Information Theory*. New York: Academic Press.

BRITTEN, P. L. & COLLINS, D. M. (1982). *Acta Cryst.* A**38**, 129–132.

COCHRAN, W. & WOOLFSON, M. M. (1955). *Acta Cryst.* **8**, 1–12.

DIAMOND, R. (1963). *Acta Cryst.* **16**, 627–639.

GASSMANN, J. (1977). *Acta Cryst.* A**33**, 474–479.

GERMAIN, G., MAIN, P. & WOOLFSON, M. M. (1970). *Acta Cryst.* B**26**, 274–285.

HAUPTMAN, H. (1974). *Acta Cryst.* A**30**, 472–476.

HEINERMAN, J. J. L. (1977). *Acta Cryst.* A**33**, 100–106.

HEINERMAN, J. J. L., KRABBENDAM, H. & KROON, J. (1977). *Acta Cryst.* A**33**, 873–878.

HENDRICKSON, W. A. & LATTMAN, E. E. (1970). *Acta Cryst.* B**26**, 136–143.

HOSOYA, S. & TOKONAMI, M. (1976). *Acta Cryst.* **23**, 18–25.

HUGHES, E. W. (1953). *Acta Cryst.* **6**, 871.

KARLE, J. & KARLE, I. L. (1966). *Acta Cryst.* **21**, 849–859.

KOENIG, D. F. (1972). *Acta Cryst.* A**28**, 55.

KOENIG, D. F. (1976). *Chem. Scr.* **9**, 14–17.

KROON, J. & KRABBENDAM, H. (1970). *Acta Cryst.* B**26**, 312–314.

LANDAU, L. D. & LIFSHITZ, E. M. (1969). *Statistical Physics*, Vol. 5, pp. 345–348. Oxford: Pergamon Press.

MAIN, P. (1976). *Crystallographic Computing Techniques*, edited by F. R. AHMED, pp. 97–105. Copenhagen: Munksgaard.

MISES, R. VON (1918). *Phys. Z.* **19**, 490–500.

MOSSEL, A. & ROMERS, C. (1964). *Acta Cryst.* **17**, 1217–1223.

NARAYAN, R. & NITYANANDA, R. (1982). *Acta Cryst.* A**38**, 122–128.

PIRO, O. E. (1977). Thesis, La Plata, Argentina.

PIRO, O. E. & PODJARNY, A. D. (1978). 36th Annual Pittsburgh Diffraction Conference, Abstract P-12, p. 35.

PIRO, O. E. & PODJARNY, A. D. (1979). Am. Crystallogr. Assoc. Winter Meet., Abstract J6, p. 76.

POST, B. (1979). *Acta Cryst.* A**35**, 17–21.

RANGO, C. DE, TSOUCARIS, G. & ZELWER, C. (1974). *Acta Cryst.* A**30**, 342–353.

SAYRE, D. (1952). *Acta Cryst.* **5**, 60–65.

SCHENK, H. (1973). *Acta Cryst.* A**29**, 77–82.

SCHENK, H. (1974). *Acta Cryst.* A**30**, 477–481.

SHANNON, C. E. & WEAVER, W. (1949). *The Mathematical Theory of Communication*. Urbana: Univ. of Illinois Press.

TSOUCARIS, G. (1970). *Acta Cryst.* A**26**, 492–499.

Acta Cryst. (1983). A**39**, 68–74

Phase Extension and Refinement by Density Modification in Protein Crystallography

BY E. CANNILLO, R. OBERTI AND L. UNGARETTI

CNR Centro di Studio per la Cristallografia Strutturale, c/o Istituto di Mineralogia, via Bassi 4, 27100 *Pavia, Italy*

(*Received* 22 *February* 1982; *accepted* 6 *July* 1982)

Abstract

A new procedure of phase extension and refinement *via* electron density modification applicable to low-resolution protein crystal structures is described. The *Sperm Whale* myoglobin structure has been used as a working molecule. The procedure of phase extension has firstly been tested starting from a set of calculated phases at 4 Å resolution; the mean phase error obtained for the 9000 strongest reflections from 4 to 1·8 Å was 39°; subsequently a mean phase error of 30° was spread into the low-resolution set and a phase refinement and extension procedure was carried out to 1·8 Å resolution. The final mean phase errors of the 1184 low-resolution model and of the 4816 strongest reflections within 1·8 Å were 22 and 50° respectively. The map calculated with this final set of reflections approaches in quality and details the map calculated with the 12 658 phases from the refined coordinates.

Introduction

A crucial step in modern protein crystallography is the calculation of a good quality electron density map of medium-to-high resolution, suitable for model building and/or least-squares refinement.

Multiple isomorphous replacement methods (MIR) very often do not achieve this goal: the crystal-

0567-7394/83/010068-07$01.50

lographer has therefore to take upon himself the laborious and time-consuming task of building and testing plausible models of the searched molecule. Even if he is supported by computer graphics he often needs additional chemical information such as the amino-acid sequence, which is not always available.

Aplysia limacina myoglobin has been studied for some years in our laboratory (Ungaretti, Bolognesi, Cannillo, Oberti & Rossi, 1978), but we never succeeded in extending resolution beyond 3·6 Å with MIR methods, owing to the failure in obtaining heavy-atom derivatives isomorphous to the native protein at higher resolution. Therefore we tried to set up a procedure for extending the low-resolution map. *Sperm Whale* myoglobin, very similar to *Aplysia* myoglobin, was chosen as a test molecule. The results so far obtained with density modification methods are reported in this paper.

Density modification is a procedure which allows the refinement of a set of existing phases and their extension to higher resolution; this aim is gained by imposing in the direct space some constraints – which may be general or peculiar to the kind of molecule under investigation – upon the electron density distribution and so modifying the starting map. By inversion of the modified map a new set of phases is obtained either for the reflections used to calculate the original map or for higher-resolution reflections, the phases of which were previously ignored. By combining the new phases calculated as above described with the observed amplitudes, a new map, containing additional structural information, can be calculated. This iterative procedure is in principle able to improve the quality of the starting phases and to increase the number of known phases.

This method was firstly used as 'phase correction' by Hoppe & Gassmann (1968) for the structure determination of small molecules. Later on it was tentatively applied to macromolecules by Barret & Zwick (1971), Collins, Cotton, Hazen, Meyer & Morimoto (1975), Collins, Brice, La Cour & Legg (1976), Raghavan & Tulinsky (1979) and Schevitz, Podjarny, Zwick, Hughes & Sigler (1981). However all these authors faced serious difficulties mainly concerned with the intrinsic limitations of the method, such as quality and resolution of the starting set of phases, and with problems in handling the critical parameters of the density modification.

In this paper we describe a density modification procedure which is easier with respect to the previous ones and apparently more suitable for refining and extending to high resolution the phases of a protein structure starting from a low-resolution model.

Two different situations have been investigated: (*a*) phase extension starting from a 4 Å resolution set of phases directly calculated from the coordinates; (*b*) phase refinement applied to a 'simulated' MIR set of phases (*i.e.* a set containing a phase-error distribution similar to that usually obtained by MIR methods), followed by phase extension from 4 to 1·8 Å resolution.

Method

A good-quality low-resolution map of a protein usually allows the distinction between regions occupied by ordered atoms and regions occupied by disordered solvent. In the papers about density modification published so far it has been assumed that the electron density (ρ) in the solvent region can be flattened to a constant arbitrary value. On the other hand, the relative heights of the peaks in the molecule region may also represent false details in the electron density and may even suggest a wrong interpretation of the map. Therefore, we have supposed that the most reasonable density modification of a protein low-resolution map, also in the molecule region, is to flatten it to a unique constant value. In particular, in our calculation we have assumed: (1) $\rho_{\text{modified}} = 1$ for $\rho >$ fixed threshold value; (2) $\rho_{\text{modified}} = 0$ for $\rho <$ fixed threshold value.

In order to evaluate the error inherent in this assumption, a 1·8 Å resulution map has been computed using the phases of the 12 658 independent reflections calculated from the refined *Sperm Whale* myoglobin atomic coordinates (Watson, 1969); hereafter these calculated phases will be called 'true'. By inversion of this map, modified according to (1) and (2), we obtained a mean phase error $\Delta\varphi = 17°$ and a residual factor $R = \sum |F_o - F_c| / \sum F_o = 0{\cdot}17$ for all the reflections. It is important to note that this error is not only intrinsically low, but also is inversely related to the amplitudes (see Table 1). Two main reasons can account for this relationship: (1) the electron density map is strongly dominated by the phases of strong reflections; (2) weak reflections are highly affected by the errors inherent to the specific electron density modification procedure applied.

Protein molecules often contain one or more metal atoms, such as iron, copper, and zinc, and the modification introduced by (1) may therefore be too drastic. The opportunity of introducing some constraints has been investigated by assuming, for instance, $\rho = 3$ instead of $\rho = 1$ for the electron density higher than 1·8 e Å^{-3} in a small volume (7·2 × 5·6 × 7·2 Å) containing the iron atom of the haem group. A slight improvement was observed in the calculated phase errors; it could probably be higher if one or more heavy atoms are present in a protein molecule. This fact suggests that heavy-atom derivatives may probably be used more successfully in a density modification procedure than the native protein.

The atomic coordinates of *Sperm Whale* myoglobin available from the Protein Data Bank (Bernstein *et al.*, 1977) were used to calculate the original set of phases and amplitudes. For the calculation of the electron

Table 1. *Mean phase error (°) and R index after inversion of the modified electron density map for 12 658 reflections within 1·8 Å resolution at various grid spacings*

Block	Number of reflections	F range	0·4 Å Phase error	0·4 Å R	0·6 Å Phase error	0·6 Å R	0·8 Å Phase error	0·8 Å R
∞–4 Å model	1184	1369–0	5·2	0·081	6·2	0·085	7·6	0·103
I	250	538–233	3·1	0·063	3·6	0·075	4·6	0·108
II	250	232–190	3·6	0·074	4·3	0·087	5·6	0·123
III	500	189–150	4·9	0·092	5·4	0·106	6·8	0·136
IV	500	150–127	5·6	0·110	6·4	0·124	8·3	0·154
V	500	127–111	6·0	0·121	7·3	0·140	9·3	0·165
VI	1000	111–88	7·1	0·140	8·2	0·160	11·6	0·200
VII	1000	88–72	8·0	0·166	9·7	0·193	13·8	0·254
VIII	1000	72–60	10·3	0·195	12·6	0·224	17·7	0·288
IX	2000	60–42	12·6	0·246	15·9	0·294	25·0	0·377
X	2000	42–27	19·3	0·336	24·8	0·391	36·3	0·518
XI	2474	27–0	44·2	0·662	49·5	0·785	59·8	1·153
Extended reflections	11 474	538–0	18·2	0·185	21·4	0·216	28·6	0·286
Overall	12 658	1369–0	17·0		20·0		26·6	

density maps a FFT algorithm (Ten Eyck, 1977) was employed.

Phase extension starting from a low-resolution model

In order to optimize the extension procedure and to verify the assumptions previously described, we started from an electron density map calculated with the true phases and amplitudes of the 1184 independent reflections from ∞ to 4 Å resolution. As expected the following parameters soon turned out to be critical: (*a*) the grid used for sampling the electron density map; (*b*) the threshold value for the boundary between $\rho = 0$ and $\rho = 1$; (*c*) the selection criteria used to accept new phases during the extension procedure.

(*a*) A considerable discussion about the maximum grid spacing which allows a good evaluation of phases and amplitudes has been reported in the literature. Several authors (Barret & Zwick, 1971; Collins *et al.*, 1975; Ten Eyck, 1977) investigated extensively the matter and finally agreed with Lipson & Cochran (1966) that: 'The number of points at which the electron density should be sampled in any one direction should be about three times the highest index observed in that direction'.

Various grid spacings were however tested between 0·8 Å (2·25 times the highest index) and 0·2 Å (9 times). The best compromise between the increase in the computing time and the accuracy of the calculated phases was reached with a 0·4 Å sampling. This grid spacing, which corresponds to *a*/162, *b*/76, *c*/88 (36, 18, 20 are respectively the highest index values), is somewhat beyond the above-mentioned prudent criterion.

(*b*) To evaluate the influence of the choice of the boundary level between molecule and solvent regions, every Fourier map was inverted several times, using different threshold values. Inspections of the different sets of calculated phases showed that the boundary level which, once chosen, reproduces most accurately the starting phases was that showing the lowest $\sum |F_o - F_c| / \sum F_o$ ratio; in particular it has been found that the best threshold corresponded to roughly 0·6 e Å^{-3} (*i.e.* only ~80 000 out of the ~540 000 grid points in one asymmetric unit needed to be considered as 'molecular' ones). A slight deviation (±10 000 points) from the best threshold value did not affect significantly the overall $F_o - F_c$ agreement and was proved to be not crucial: once it has been chosen, few cycles of extension converged to a mean phase error very near to that obtained by working with the original best threshold.

(*c*) As for the strategy of phase extension it was found that the crucial point was to arrange the reflections between 4 and 1·8 Å in order of decreasing amplitude instead of increasing resolution. Then small blocks of reflections were added successively in every step of the procedure to the already phased set. It was found that every addition of 'new' reflections (even if some of them were badly phased) reduced the phase errors of the reflections previously extended. After some additions, it turned out that a great improvement could be obtained by selecting the extended reflections with lowest phase errors and using them to calculate the next map. The best selection criterion was found to be $R = |F_o - F_c|/F_o$, which was, on average, correlated with the phase error, particularly for the reflections of strong–medium intensity. The electron density map shows in fact significant changes when the phases of strong reflections are changed and this in general determines large variations in the calculated amplitudes. If the worst-phased reflections (*i.e.* those with $R > 0{\cdot}30$) were excluded, a map which allowed the

calculation of new and, on the average, better phases for the excluded reflections was obtained. This procedure was iterated for a few cycles.

Moreover we found that it was very useful, after the inclusion of several extended reflections (*e.g.* 5000), to start the procedure again by using only the model and the first block containing the strongest extended reflections.

This kind of procedure converges quite quickly with a small phase error for the extended reflections: if the 1184 reflections within 4 Å resolution are used as the starting model, with the phases constrained to the true values, 9000 extended reflections within 1·8 Å resolution can be phased with a mean phase error of 20, 26, 32, 39° respectively for the first 3000, 5000, 7000, 9000 reflections arranged in order of decreasing amplitude. At the end of the extension procedure the calculated phases for the 4 Å model differ by ~9° on the average from the true values. The resulting electron density map is fairly equivalent to the map calculated with the true phases and its interpretation is easy and straightforward.

Phase refinement and extension

Once strategy and parameters for the phase extension procedure had been optimized, they were applied to a set of data which simulated an experimental one. A good 4 Å resolution MIR map has usually a mean figure of merit (f.o.m.) around 0·85 corresponding to a mean phase error of 30°. As a consequence of the MIR phasing procedure, this error is more heavily distributed on weaker acentric reflections, especially on those of higher resolution. Accordingly a mean phase error of 30° was spread in the 4 Å resolution model of *Sperm Whale* myoglobin with a distribution against intensity and resolution of the reflections nearly equivalent to that obtained with MIR methods for the *Aplysia limacina* myoglobin. An individual f.o.m. equal to *cos* (*phase error*) was applied to every reflection for phase error <90° and a f.o.m. equal to 0 was applied for phase error >90°.

It was soon clear that the phase extension procedure described above did not yield good enough results, if applied as with a set of true phases. The phase error present in the low-resolution model was heavily propagated into the new calculated phases.

However, it was realized that there was a definite possibility of reducing the starting phase errors. A kind of phase refinement was therefore applied, by subsequent calculations and inversions of the low-resolution starting map, firstly calculated only with reflections within 4 Å, and successively also with the 500 more intense extended reflections. As can be inferred from Table 2, a good improvement was obtained in the first cycle, especially for the strong reflections initially affected by great phase error. This fact shows how the modification and inversion of an electron density map can improve the MIR phases in protein crystallography. Furthermore, small blocks of reflections within 4 Å resolution with a definite amplitude range (*e.g.* 300–250, 250–200) were excluded for one cycle and then their phases and amplitudes were calculated again. This treatment is a kind of selection, like that shown in the previous paragraph for the extended reflections. In this way we obtained a lower and more favourable error distribution in the starting set. Even if the overall mean phase error has decreased only by a few degrees, the Fourier map, which is mainly dominated by the strong reflections, was considerably improved.

The slight improvement of the low-resolution phases during the last cycle of refinement (see cycle 7 in Table

Table 2. *Distribution of the mean phase error* (°) *in the* 4 Å *model during the refinement and extension procedure*

F range	Number of reflections	Starting set	Cycle 1	Cycle 7	Cycle 35
>200 with f.o.m. <0·85	329	54·3	35·8	28·6	†
>200	688	30·7	22·3	18·9	17·6
<200*	496	28·7	41·6	34·7	33·4
Overall	1184	29·9	30·3	25·5	24·2
Working set	1184	29·9	25·0	23·0	22·2

* It was found that the method does not yield good phase values for weak low-resolution reflections if applied before extension: so the initial phases were used for this group of reflections. Together with the current phases of the reflections with $F > 200$ they made up the working set of phases.

† During the extension procedure f.o.m.'s up to 1·0 were attributed to the reflections; therefore most of this class of reflections were promoted to f.o.m. > 0·85.

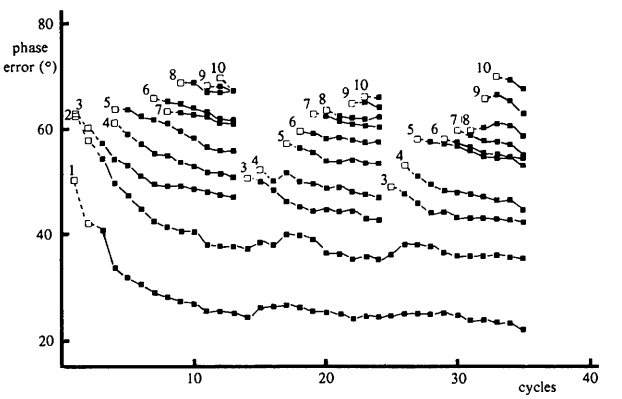

Fig. 1. Mean phase error (°) *vs* number of cycles of phase refinement and extension for blocks of extended reflections between 4 and 1·8 Å. Peculiarities of each block are defined in Table 3. Empty squares refer to the phase error for reflections which were not yet inserted in the calculation of the Fourier map. See text for further details.

2) suggested that we begin to exploit the information included in the extended reflections.

The phase extension procedure was then applied as described above. The starting f.o.m. was firstly maintained for the resolution model, then recalculated on the basis of the R index for individual reflections: this was done at first only for the reflections with f.o.m. $<0\cdot85$ and subsequently for all of them. A f.o.m. proportional to R was also attributed to the extended reflections, on the basis of the following R ranges: f.o.m. = 1·0 for the reflections with $R < 0\cdot1$, 0·9 for $R < 0\cdot2$, 0·8 for $R < 0\cdot3$, 0·6 for $R < 0\cdot4$, 0·5 for $R < 0\cdot5$, 0·3 for $R > 0\cdot5$. The state of the phase refinement and extension procedure is monitored in Fig. 1, which refers to the phase errors of the ten blocks in which all the extended reflections have been arranged according to their amplitude. Cycle 1 is the first modification and inversion of the 4 Å electron density map; cycles 2–4 refer to the refinement of the model by means of additions of three blocks containing the strongest 566 reflections; cycles 5–7 to the refinement by means of 'selections' in the model; cycles 8–13 to the extension procedure up to a total of 6000 reflections. Cycles 14–24 refer to the extension procedure from a new starting set made up of the 4 Å resolution refined model and the first two blocks of extended reflections. Cycles 25–35 are only a repetition of cycles 14–24. The phase-error distribution in cycles 13, 24 and 35 is shown in Table 3. It is quite clear that the improvement obtained in cycles 25 to 35 is very small compared to that of the previous iteration, suggesting that the procedure has reached convergence, at least under the present conditions.

Furthermore, the high value for the phase error of the very weak reflections (see *e.g.* block 10) dissuades one from going on with the extension procedure towards lower amplitudes. However, this is not a crucial drawback because the Fourier map of a protein molecule is dominated by the strongest reflections. This can be seen in Fig. 2 where four sections of the electron density map calculated with (*a*) the true phases of 12 658 reflections within 1·8 Å and (*b*) the 4 Å model and the 4816 strongest reflections are reported.

The meaning of the phase errors obtained with this procedure can be evaluated by inspection of the final electron density map. Fig. 3 shows the comparison between (*a*) the original 'best Fourier' at 4 Å resolution, (*b*) the 1·8 Å resolution map calculated with phases and f.o.m. of the 1184 + 4816 = 6000 reflections refined and extended as described above, (*c*) the 1·8 Å resolution map calculated with the true phases of the same 6000 reflections, and (*d*) the 4 Å resolution map calculated with the true values for low-resolution phases. The atomic positions of the non-hydrogen atoms are dotted in order to expedite the interpretation of the electron density. Map (*b*) is very similar to (*c*) and it looks greatly improved in comparison with (*a*). It is worthwhile noting that the changes of the electron density during the process are always in the direction of the 1·8 Å true map. Many of those modifications are not foreseeable from the 4 Å true map and have been therefore purely determined by the phase extension procedure.

Table 3. *Mean phase error (°) for extended reflections during the extension procedure*

Block	Number of reflections	F range	Cycle 0*	Cycle 13	Cycle 24	Cycle 35
4 Å model	1184	1369–0	29·9	23·0	23·1	22·2
1	116	538–279	42·1	25·0	24·6	21·9
2	200	279–220	57·9	37·4	35·6	35·5
3	250	220–184	60·2	47·3	42·7	42·3
4	250	184–162	61·2	50·4	47·1	43·9
5	500	162–134	64·0	55·8	53·6	52·8
6	500	134–116	65·9	61·4	57·6	53·4
7	500	116–103	63·4	60·4	60·6	54·4
8	500	103–92	69·1	67·7	62·5	58·1
9	1000	92–75	67·9	67·6	64·7	63·9
10	1000	75–62	69·7	67·5	66·4	68·4

* Mean phase error before the insertion in the Fourier map calculation.

(*a*)

(*b*)

Fig. 2. Sections of the electron density map between $z = 0\cdot87$ and $z = 0\cdot96$ calculated with: (*a*) the 12 658 independent reflections to 1·8 Å resolution, (*b*) the 4 Å model and the 4816 strongest reflections of the 1·8 Å set of data. Only one independent molecule has been reported.

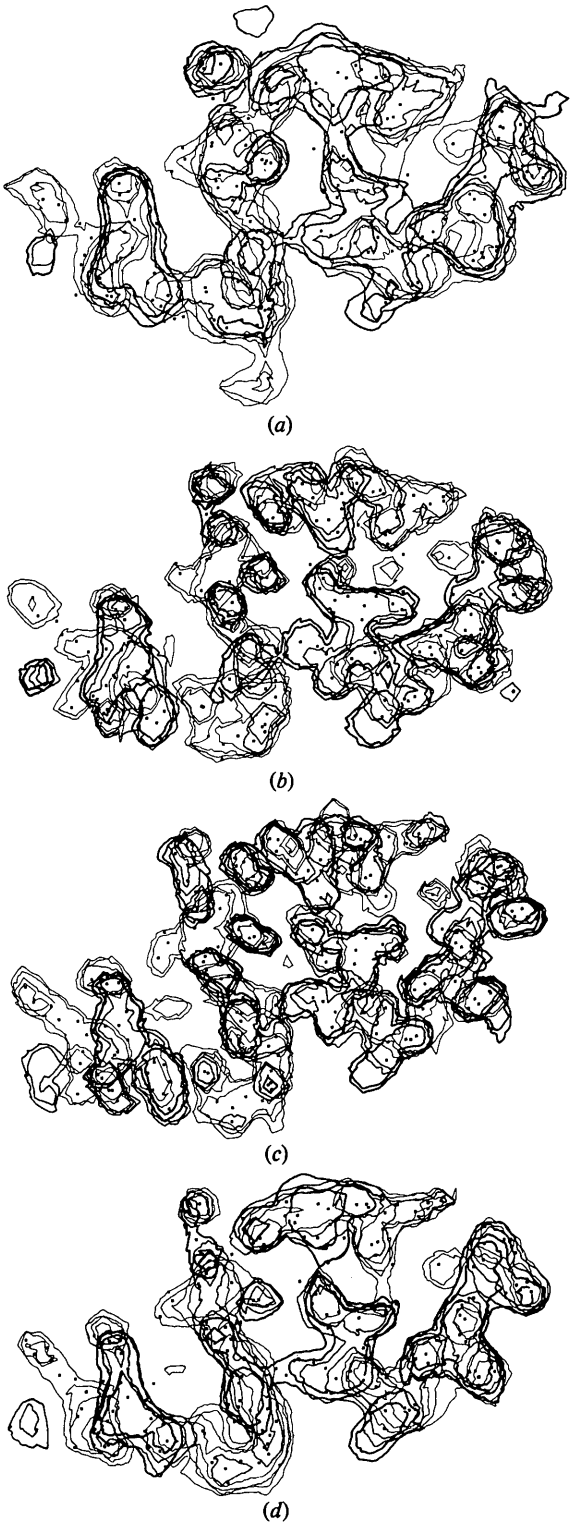

Fig. 3. The same sections of the electron density map as in Fig. 2 from: (*a*) the 4 Å original map (mean phase error $\Delta\varphi = 30°$), (*b*) the final extended map calculated with the 4 Å model and the 4816 more intense reflections within 1·8 Å, (*c*) the theoretical map obtained with the true phases of the previous reflections, (*d*) the theoretical 4 Å map.

Conclusion

The density modification procedure described in this paper, if applied to a correct low-resolution map, allows one to obtain good and straightforward results. If the original low-resolution phases are strongly affected by experimental errors, the potentiality of the method is reduced. However, iterative cycles of refinement of the model and of phase extension are able to produce fairly good results which allow one to solve all the ambiguities which are present in the interpretation of the original 4 Å best Fourier map; moreover, many significant details, due to the increased resolution, are added. This situation allows one to build quite easily a molecular model of the protein and to undertake least-squares refinement.

The advantages of this kind of procedure are evident: no preliminary knowledge of the amino-acid sequence and/or structural details are needed. The human interference is kept to a minimum; typically it may be enough to choose the threshold value of ρ and R in order to make a not too drastic selection.

On the other hand, every kind of known structural detail may be added as an additional constraint of the density modification. In our case, for instance, we have used $\rho = 3$ for a limited number of points around the position of the haem of the myoglobin molecule determined from the low-resolution MIR map.

First attempts to apply this procedure to *Aplysia* myoglobin MIR data are now in progress. Phases up to 2·8 Å resolution have been in the meanwhile obtained in our laboratory starting from the 3·6 Å MIR map by applying energy and crystallographic refinement with the program written by Jack & Levitt (1978). In this way about 80% of non-hydrogen atoms have been placed in the electron density map. We expect it will be possible to make in a short time a comparison between and two sets of phases in order to evaluate the advantages and deficiencies of the two procedures.

We would like to thank G. Germani for his help in various computational problems throughout this work.

References

BARRET, A. N. & ZWICK, M. (1971). *Acta Cryst.* A**27**, 6–11.

BERNSTEIN, F. C., KOETZLE, T. F., WILLIAMS, G. J. B., MEYER, E. F. JR, BRICE, M. D., RODGER, J. R., KENNARD, O., SHIMANOUCHI, T. & TASUMI, M. (1977). *J. Mol. Biol.* **112**, 535–542.

COLLINS, D. M., BRICE, M. D., LA COUR, T. F. M. & LEGG, M. J. (1976). In *Crystallographic Computing Techniques*, edited by F. R. AHMED, K. HUML & B. SEDLACEK, pp. 330–335. Copenhagen: Munksgaard.

COLLINS, D. M., COTTON, F. A., HAZEN, E. E. JR, MEYER, E. F. JR & MORIMOTO, C. N. (1975). *Science*, **190**, 1047–1052.

HOPPE, W. & GASSMANN, J. (1968). *Acta Cryst.* B**24**, 97–107.

JACK, A. & LEVITT, M. (1978). *Acta Cryst.* A**34**, 931–935.
LIPSON, H. & COCHRAN, W. (1966). *The Determination of Crystal Structures. The Crystalline State*, Vol. III, p. 103. London: Bell.
RAGHAVAN, N. V. & TULINSKY, A. (1979). *Acta Cryst.* B**35**, 1776–1785.
SCHEVITZ, R. W., PODJARNY, A. D., ZWICK, M., HUGHES, J. J. & SIGLER, P. D. (1981). *Acta Cryst.* A**37**, 669–677.
TEN EYCK, L. F. (1977). *Acta Cryst.* A**33**, 486–492.
UNGARETTI, L., BOLOGNESI, M., CANNILLO, E., OBERTI, R. & ROSSI, G. (1978). *Acta Cryst.* B**34**, 3658–3662.
WATSON, H. C. (1969). *Prog. Stereochem.* **4**, 299–333.

Acta Cryst. (1983). A**39**, 74–76

On Colored Lattices and Lattice Preservation

BY MONIQUE ROLLEY-LE COZ

Département de Mathématiques, Faculté des Sciences et Techniques, 6, avenue Le Gorgeu, 29283 Brest, France

MARJORIE SENECHAL

Department of Mathematics, Smith College, Northampton, Massachusetts 01063, USA

AND YVES BILLIET*†

Département de Chimie, Faculté des Sciences et Techniques, 6, avenue Le Gorgeu, 29283 Brest, France

(*Received* 1 *April* 1982; *accepted* 20 *July* 1982)

Dedicated to Dr David Harker on the occasion of his 75th birthday

Abstract

Two questions which have been independently studied (the distribution of colors in colored lattices and lattice preservation in derivative lattices) are in fact closely related. It is possible, for instance, to determine the distribution of colors in rows and nets by the lattice-preservation indices c_r and c_p as functions of row indices $[u_0,v_0,w_0]$ and net indices (h_0,k_0,l_0), respectively. A formula is also given for the number of classes of equivalent derivative lattices of a given index n.

1. Introduction

Recently two questions have been studied independently:

(1) The distribution of colors among the lattice points or nodes in the rows and the nets of a colored lattice L^c (Harker, 1978).

(2) The preservation of the lattice nodes by the rows and the nets of a derivative lattice (sublattice) L' of a lattice L (isomorphic subgroup of $P1$) (Billiet, 1979; Rolley-Le Coz & Billiet, 1980, 1981).

In fact these questions are closely related. Every derivative lattice can be identified with a colored lattice L^c and *vice versa*. We assign a single color to the nodes of the derivative lattice L'; the cosets of L', with respect to L, correspond to different colors. Every translation of the colored lattice L^c by a vector of L' leaves the color distribution in the lattice L^c unchanged, whereas a translation by an element of each of the cosets of L' corresponds to a certain color permutation, the same permutation for all members of a coset. The number n of distinct colors is equal to the index of L' in L. Conversely, the nodes of L^c with a single color define a derivative lattice L'.

In this paper we combine our efforts to clarify such misunderstood points as the distribution of colored nodes *as a function of the indices* of rows and nets. For definitions and terminology, the reader is referred to the previous papers.

2. Colored nodes and derivative lattices

Let L be a three-dimensional lattice and L' a sublattice of L of finite index. Primitive unit cells (a_0,b_0,c_0) of L and (a'_0,b'_0,c'_0) of L' may always be chosen in such a way that their vectors are related by the simple equations $a'_0 = fa_0$, $b'_0 = fgb_0$, $c'_0 = fghc_0$. Here f, g and h are positive integers whose values are unique for a

* To whom all correspondence should be addressed.
† Present address: Institut des Sciences Exactes, Université de Sétif, Sétif, Algeria.

0567-7394/83/010074-03$01.50